EPJ Web of Conferences **87**, 02017 (2015)
DOI: 10.1051/epjconf/ 20158702017

Feedback-controlled NTM stabilization on ASDEX Upgrade

J. Stober[1,a], L. Barrera[1], K. Behler[1], A. Bock[1], A. Buhler[1], H. Eixenberger[1], L. Giannone[1], W. Kasparek[2], M. Maraschek[1], A. Mlynek[1], F. Monaco[1], E. Poli[1], C.J. Rapson[1], M. Reich[1], M. Schubert[1], W. Treutterer[1], D. Wagner[1], H. Zohm[1], and the ASDEX Upgrade Team[1]

[1] *Max-Planck-Institut für Plasmaphysik, Garching, Germany*
[2] *Institut für Grenzflächenverfahrenstechnik und Plasmatechnologie (IGVP), Universität Stuttgart, Stuttgart, Germany*

Abstract. On ASDEX Upgrade a concept for real-time stabilization of NTMs has been realized and successfully applied to (3,2)- and (2,1)-NTMs. Since most of the work has meanwhile been published elsewhere, a short summary with the appropriate references is given. Limitations, deficits and future extensions of the system are discussed. In a second part the recent work on using modulated ECCD for NTM stabilisation is described in some detail. In these experiments ECCD power is modulated according to a magnetic footprint of the rotating NTM. In agreement with earlier results it could be shown that O-point heating reduces the necessary average power for stabilisation whereas X-point heating hampers stabilisation. Although this modulated scheme is not relevant for routine NTM stabilisation on ASDEX Upgrade it may be mandatory for ITER or DEMO. On ASDEX Upgrade it has been re-developed to demonstrate the usage of a FAst DIrectional Switch to continously heat the O-point of the rotating island with only one gyrotron switching between two launchers which target the mode at locations separated in phase by 180 degrees as described in [1].

1 Introduction

Neoclassical-Tearing-Modes (NTMs) are helical structures in a toroidal equilibrium. They exist on surfaces with rational q-values where they form islands which short-cut the thermal insulation. These modes are characterised by a marginal island width below which the mode disappears on its own and above which it grows with a rise time of the order of τ_E until it reaches the saturated island width which characterises the detrimental effect of the fully developed island. Driving terms are the pressure gradient and the magnetic shear at the resonant surface. The mode can be removed (stabilised) by driving a current inside the island or its appearance can be completely avoided by preemptive current drive. Since a finite island size is needed for the mode to grow, the mode does not reappear immediately after stabilisation when switching off the ECCD. The balance between stabilizing and driving terms determines how large a seed island is necessary. For strong driving terms and correspondingly small initial island sizes, permanent preemption will become more economical than intermittent stabilisation, since less current drive is needed for preemption (the current on the flux surface is only enforced, it is not necessary to over-compensate a helical hole in the current profile) as has been demonstrated theoretically and experimentally. Still the stabilisation of an existing NTM is initially the easier task since the NTM spinning toroidally with the plasma leads to characteristic disturbance of radially resolved electron temperature profiles, thereby revealing where to drive the additional current. For preemption the position of the resonant surface has to be deduced from the magnetic equilibrium only.

The saturated island width can have a radial width of 10-20% of the minor radius, the marginal width is a few %. In order to drive the majority of the current inside an island close to the marginal width, the width of the driven current profile should be of similar size or smaller. Such localised currents can so far only be driven using ECCD. For ITER the request on the ECCD width may be fulfilled only marginally especially when taking into account a potential broadening of the beam due to density fluctuations [2]. Under these circumstances the amount of current driven outside the island must be minimised by modulation of the beam with respect to the O-point of the rotating island.

This contribution consists of two main parts. First we summarize the status of the real-time NTM-stabilisation project on ASDEX Upgrade which has been a long-standing topic in the past workshops of this series. The successful application of the feedback-control and its com ponents has been described in several conference contributions and journal papers. This has been a major part of the poster at the workshop but is here only shortly summarized in section 2 in order to minimize repetitions from other sources which the interested reader has to read anyway to get a detailed picture. In the second part we address the issue of O-point heating with a modulated beam, which is not necessary for regular NTM-control on AUG since the ECCD width is sufficiently small but may be

[a] e-mail: Joerg.Stober@ipp.mpg.de

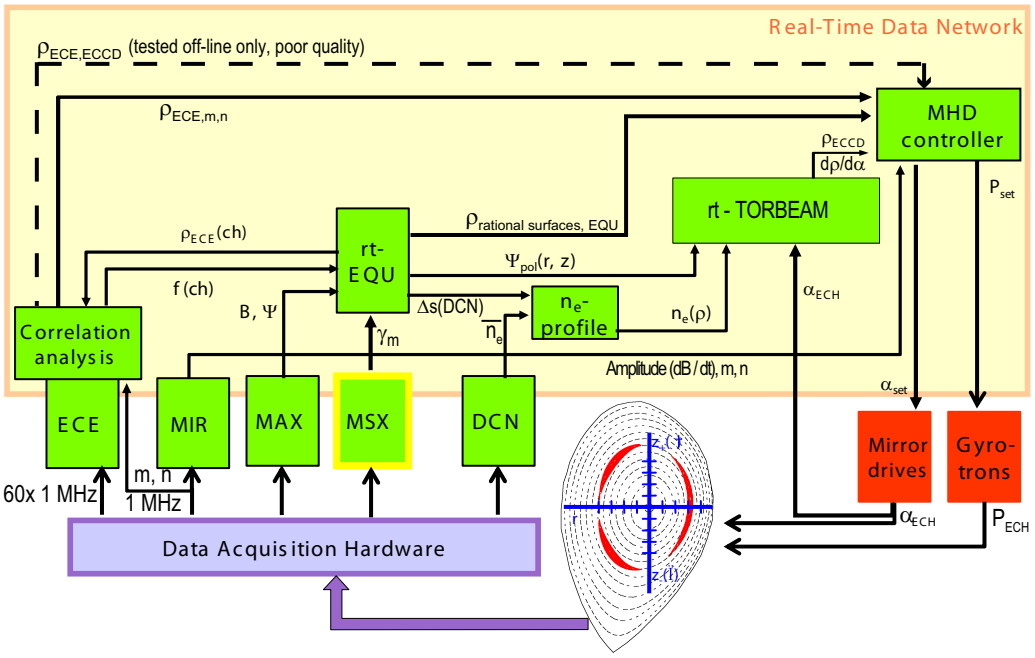

Figure 1. Schematic overview of the real-time MHD-control frame work set up at AUG. Green boxes correspond to real-time data evaluation with different levels of complexity. All except the MHD-controller use the rt-diagnostic concept [3, 4], i.e. they run as autonomous units exchanging input and output with the discharge control system (DCS) and other rt-diagnostics via a rt-data network. This network operates in an asynchronous mode and is mainly limited by 1GB/s Ethernet-switches. All data are transfered with a time stamp. The MHD-controller itself is part of the DCS. The yellow frame around MSX visualizes the fact that the MSE-system is not yet a reliably working rt-system.

necessary for ITER or even more for DEMO. The main motivation to take the O-point modulation up again is the FAst DIrectional Switch (FADIS) installed in the AUG-ECRH-System. By fast frequency tuning of the gyrotron this microwave interferometer allows to switch the beam between two launchers [5]. Especially if a device has more launchers than gyrotrons (such as ITER) a FADIS allows to switch the power of one gyrotron between two launchers aimed such that they hit the O-point of the mode with a phase difference close to 180 degree. This would allow to make most efficient use of the ECCD for NTM-stabilisation. In section 3 the on/off-modulation with one gyrotron and one launcher is described in some detail. Even with the rather narrow beam a beneficial effect of O-point modulation is observed. The FADIS experiments are described in [1].

2 Feedback controlled NTM-stabilisation

The concept, realization and feedforward-testing of the separate components of the NTM-stabilisation system have been described at the two previous work shops of this series [6, 7] and references therein. In the following this is summarized including more recent references. For illustration a schematic overview is given in figure 1. Reliable mode detection and identification is achieved by a linear combination of Mirnov-pick-up-coils to generate a specific $|\dot{B}|$ signal for a specific low-order (m, n)-combination. If the amplitude of the signal for any of the implemented m,n combinations exceeds a certain threshold the respective mode is considered to be present in the plasma. By correlating all fast ECE channels separately with this characteristic signal the mode related content of the T_e fluctuations is extracted and the expected radial phase jump in these fluctuations can be determined and is assigned to the mode position [8]. Initially the result is a fractional ECE-channel-number which can be translated into a rho-value using the real-time equilibrium [9] and the ECE-optics. Since the ECE-antenna is located at the outboard mid-plane and the optical axis is almost perpendicular to the flux surfaces (at least up to half radius where the NTMs are located) we neglect (so far) any bending of the ECE-viewing-geometry by density gradients. This detection is robust unless the mode width is too small, which in our applications so far is typically smaller than the marginal island width. Alternatively the respective resonant flux-surface can be determined directly from the equilibrium searching for the respective $q = m/n$. Unfortunately both results are in practical applications not necessarily identical. The location of a rational surface depends crucially on the profile of the plasma current. Therefore the reliable determination of the resonant flux surface from the equilibrium reconstruction can either be achieved using sufficiently accurate diagnostics of the current profile (motional Stark effect or polarimetry) or by optimizing the bias current profile of the reconstruction for the plasma under

study, for example in a sequence of discharges where the mode position was determined by ECE.

The fundamental task of the feedback control is to adjust the ECRH launchers such that the maximum of the driven current lies on the same flux surface where the mode has been located. To do so the control system has to know the actual position of the driven current in ρ as a function of the actual launcher angle α of the ECCD and its rate of change as α is changed, i.e. $d\rho/d\alpha$. Due to the cylindrical shape of the resonance and the toroidal shape of the flux surfaces with variable elongation the relationship is not necessarily trivial. $\rho(\alpha)$ and its derivative are calculated via ray tracing using a simplified version of the TORBEAM-code [10] neglecting beam broadening and current drive. Implicitly we assume here that the maximum of the driven current is sufficiently close to the maximum of the heating determined by the single-ray real-time version. This has been verified for the experimental scenario under study comparing with results from the full-beam version of TORBEAM. The derivative is obtained from three runs with slightly different values of α. In AUG we use for these experiments up to 4 ECRH Launchers with different geometries in the sense that separate $\rho(\alpha)$ relations have to be determined for each launcher. Therefore we calculate in parallel 12 rays on a common equilibrium within 30 ms. The TORBEAM calculation requires a sufficiently accurate density profile which is obtained in real-time from 5 interferometer channels and their paths lengths through the plasma. The latter are determined from the equilibrium supplied by the real-time equilibrium solver [9, 11]. Initially an alternative method to determine the ECCD deposition was envisaged by modulation of the ECCD power and a correlation of the power signal with ECE. During off-line testing it became obvious that this concept was not feasible with the necessary resolution in space and time as indicated by the dashed arrow in figure 1.

The feedback control experiments in the last 2 years optimized the control of the ECCD launchers to adjust the ECCD profile on the resonant surface. By doing so (3,2)- and (2,1)-NTMs were stabilized within a few energy confinement times τ_E [12]. The major principal difficulties arise from flux surface mapping (the ECE measures at the outboard mid-plane, the ECCD position is at the top or bottom of the flux surface) and uncertainties in the density profile and consequently in the ECCD deposition. These effects may lead to an offset between the mode- and the ECCD-location of up to 2 cm which is in the order of the beam width of approx 3 cm such that the modes are not always fully stabilized. Unfortunately there has so far no systematics been detected in the offset. In such a situation one needs refined strategies to achieve a full stabilisation. On AUG an offset can be included into the control. This offset (which is assumed to be constant for all launchers) can be adjusted in real-time minimizing the mode amplitude. With this scheme, complete stabilisation has been achieved [13], but the statistics (i.e. number of tests) is still low. Further refinements are tested in the ongoing campaign. The mode signal is not launcher-specific such that separate offset-corrections for each launcher were not attempted yet. As an alternative the applicability of in-line ECE is studied [14] on AUG which would ideally allow a launcher specific fine adjustment on the position of the phase jump.

As mentioned above preemptive ECCD may be the best choice for frequently reappearing NTMs. First experiments [9] demonstrated successful preemption, but not with sufficient reliability, mainly due to uncertainties in the current profile as discussed above, since the MSE-system on AUG does not yet deliver reliable real-time data. Further experiments using an improved bias of the current profile and a refined mirror control are part of the ongoing AUG campaign.

3 NTM stabilisation with modulated ECCD

The use of mode-locked power modulation in case the ECCD profiles are significantly broader than the marginal island width has been pioneered in AUG [15]. It was shown that widening of a cw-beam hampered full stabilisation of the NTM, which could be regained using O-point modulation (roughly 50% duty cycle). X-point modulation was less stabilizing (in terms of the minimum achieved mode-amplitude) than cw.

In these old experiments ECCD was driven at the high field side (HFS) of the resonant flux surface where $\vec{k}$ is almost perpendicular to the flux surface. Beam broadening was achieved by varying the toroidal inclination. Due to the corresponding Doppler broadening the deposition profile was broadened in the direction of ρ. ECCD widths of $\Delta\rho \approx 0.2$ have been obtained. Since 2007 AUG operates with W-covered plasma facing components. Typically the scenarios which develop NTMs (H-modes with moderate density and moderate q_{95}) are prone to detrimental W-accumulation in the plasma center unless significant electron heating is applied in the plasma center. Most effective is central ECRH with the resonance close to the axis. This means that the same frequency cannot be used for NTM stabilisation on the HFS, but the NTM has to be stabilized at $R = R_0$ at the top or bottom of the flux surface. In [6, 16] this has been discussed in detail. The consequence with respect to experiments with modulated ECRH is that beam broadening can no longer be generated by increasing the toroidal inclination since the Doppler shift now broadens the deposition tangentially to the flux surface such that there is essentially no broadening in ρ. Similar widths as in the old experiments cannot be obtained anymore. Modifications of the launcher-mirror surfaces to defocus the beam are a possibility to continue in this direction, but this would obviously influence a whole campaign. For this reason NTM stabilisation with modulated ECCD was somewhat out of focus at AUG in the last years.

Recently the topic has gained new interest in combination with the FAst DIrectional Switch (FADIS [1]). It is proposed to use such a switch to make more effective usage of the installed ECRH power in ITER in case modulated ECCD is necessary for NTM stabilisation. Since ITER has more launchers than gyrotrons one could use one

gyrotron with two launchers and point the launchers such that the mode passes the two deposition regions ≈180 ° out of phase. Finally, using FADIS, the gyrotron power is switched in phase with the mode between both launchers, such that the power is always injected close to the O-point (i.e. within [-90°,+90°]). As described in [1] a demonstration was attempted at AUG. In preparation, the locking of the ECCD to the rotating mode in a well defined phase has been reestablished and some stabilization tests have been performed. Figure 2 shows that they were successful and well in line with the previous results. The ECCD deposition was scanned across the resonant surface twice by a pre-programmed rotation sequence for one launcher axis. For cw-operation and dominant O-point heating the mode disappeared during the first crossing, roughly at the ρ-value expected from RT-Torbeam, the ECE-NTM-location and the estimated position of the (3,2)-surface. With dominant X-point heating the mode was not fully stabilized. In the latter case the mode amplitude has two minima in the vicinity of the two expected crossings. CW-power is 700kW, the time-average power for O-point modulation is 410 kW. We did not do further study the minimum power for complete stabilisation with cw and O-point modulation. Since CW can be regarded as a mixture of X- and O-point modulation it seems likely that the threshold for the time averaged power should be somewhat lower for the O-point modulation. As described in [1] the FADIS experiments were so far hampered by difficulties in resonator tuning and launcher setting and did not show complete suppression although the average power was ≈500 kW. Using the improved NTM-location algorithms and an optimized resonator tuning full NTM stabilisation with 'permanent O-point heating' using FADIS may be demonstrated later in the ongoing AUG-2014-campaign.

We end this section addressing some of the technical issues related to the modulation in phase with the O-point. As discussed already in [15, 17] there is an intrinsic phase delay between the Mirnov signal and the ECCD modulation due to two independent effects. The O-point corresponds to the zero of $\dot{B}_R$ where the sign of $\dot{B}_R$ changes from positive to negative, resulting in a phase difference of 90° between the maximum of $\dot{B}$ and the center of the ECRH-on interval. An additional phase difference arises when taking account of the different locations of ECCD and $\dot{B}$ measurement on the flux surface as discussed in detail in above mentioned references. Adding the two phases with the correct signs results in a phase difference which has to be technically realized with the gyrotron. On AUG one period is ≈40-60 μs (15-25 kHz), an accuracy of 1 μs is required to achieve a phase match better than 10°. The time for Mirnov data acquisition, analogue linear combination and transmission via 100 m of optical fibre is estimated to be faster than 100 ns. The latter step consists of a voltage-frequency converter (10 MHz ± 1 MHz corresponds to ± 10 V). The frequency is transmitted through the glass fibre by light flashes and back converted to a voltage on the other side. A transmission time below 100 ns has been explicitly verified using two independent data loggers on both ends of the optical fibre (analogue input versus ana-

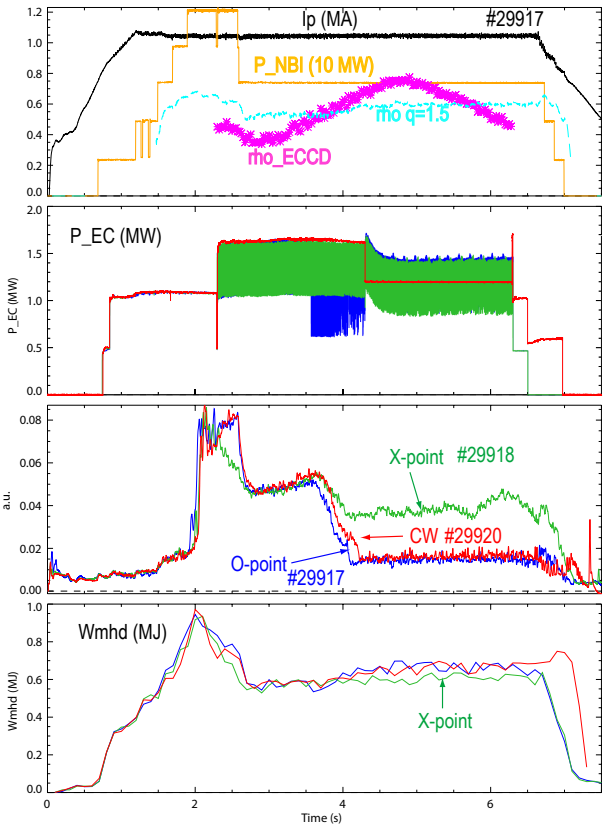

Figure 2. Comparison of three discharges with identical control parameters, except the modulation scheme. The latter was 50% duty cycle, close to O-point (#29917), 50% duty cycle, close to X-point (#29918) and 100% duty cycle, i.e. CW (#29920). The upper box shows the scenario (all time traces in this box from #29917 as typical example): In the 1 MA discharge, a (3,2) NTM is triggered by a fast increase of the NBI-heating to 12.5 MW. One axis of the EC-launcher is pre-programmed to sweep the ECCD-deposition (here from real-time TORBEAM) accross the resonant surface (here for the real-time equilibrium). The box second from top shows the EC power. The modulation phase is clearly seen. For the O-point case one of the underlying centrally-heating CW-gyrotrons was lost at ≈ 3.5 s, but the off-axis modulation worked as planned. The box second from bottom shows the upper envelopes of the $\dot{B}$ signals of the Mirnov coils. As described in the text, a linear combination of several coils is used to represent as close as possible the even n, odd m content. For the O-point and CW cases the mode is stabilized close to the time point when the deposition crosses the resonant surface. Also in the X-point case the mode amplitude is reduced but the mode is not fully stablized. A second minimum of the mode amplitude is observed at the second crossing of deposition and resonant surface. At the bottom the stored energy is shown. As expected it reaches higher values for the cases when te NTM is fully stabilised. Note that the NBI heating in this phase of the discharges has been reduced to 7.5 MW such that a full recovery of the maximum stored energy cannot be expected.

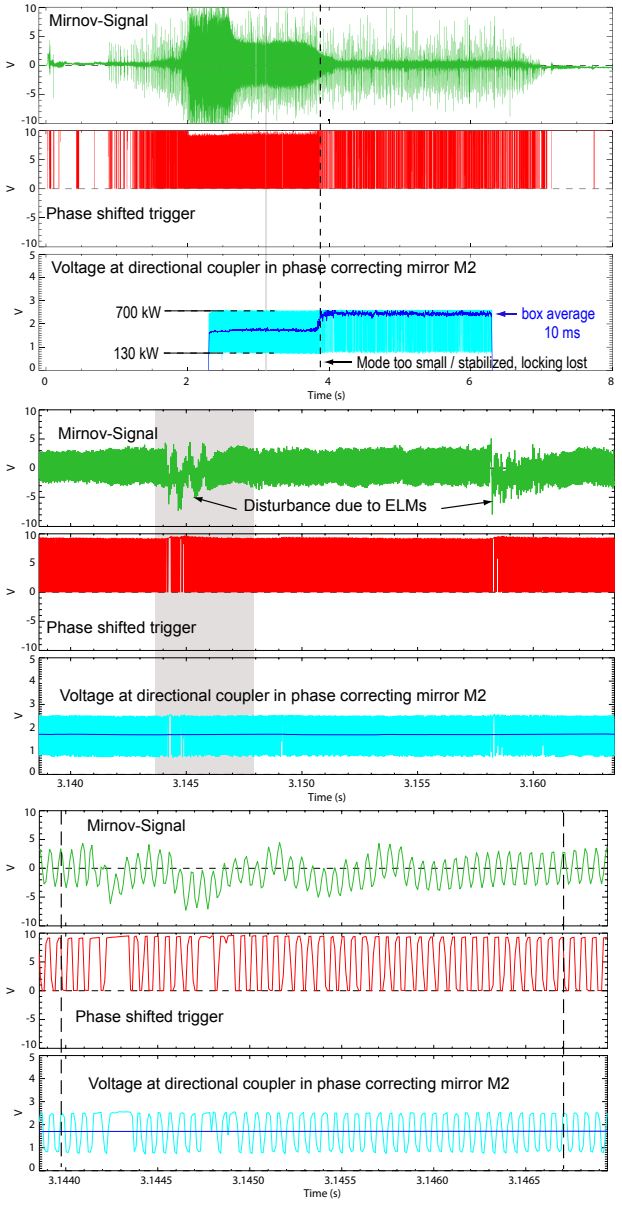

Figure 3. Time traces related to the mode locked injection of ECCD (AUG discharge #29917 in fig. 2). Middle: zoom into the top-traces (x 240). Zoomed time interval shaded in grey in top part. Bottom: zoom into the middle traces (x6), zoomed interval is shaded in middle part. The dashed vertical lines are added to see the phase differences at two arbitrary time points. Each of the three zoom-states consists of three time traces. Top (green): $\dot{B}$ from Mirnov coils linearly combined to correspond to odd m, even n. Middle (red): Output of the phase shifting unit. Bottom (cyan, blue): Voltage at the directional coupler embedded in the second phase correcting mirror M2 of the matching-optics unit. Blue is a sliding box average over 10 ms.

logue output), both triggered by the optical-fibre based AUG trigger system. These small time-shifts are neglected in the following. An FPGA-based phase shifter converts the Mirnov-Signal into phase-shifted trigger-pulses for the series-tube modulator. During the low-period of the trigger the modulator reduces the acceleration voltage of the electron beam in the gyrotron by a pre-set value. In the case shown here from -41.5 kV to -28.5 kV (constant depression +32 kV) resulting in a reduction of the power from 700 kW to 130 kW. Data transmission to the series modulator uses a digital optical transmission which introduces a fixed delay of 18 μs. This results in an uncomfortable procedure to achieve the requested phase delay between Mirnov-signal and ECCD: Based on the expected frequency of the mode, the 18 μs are converted into a phase difference which is subtracted from the requested phase difference. The result is then set at the phase shifter (using a potentiometer) with the help of a function generator and an oscilloscope. Additionally the trigger level has to be set at the phase shifter (with another potentiometer) in order to prevent triggering on noise without losing too much sensitivity on real modes. If the real frequency differs from the expected frequency this leads to an improper phasing. In the examples shown here a mode frequency of 22 kHz was expected and the real frequency finally was 15 kHz (during the experiments it was decided to use one NBI source less). Therefore the center of the on-intervals are in fact at 45° (O-point heating) and 225° (X-point heating) with respect to the O-point, i.e. shifted by 45°. In principle such problems could be avoided by inclusion of the fixed delay of 18 μs into a more complex FPGA program for the phase shifter if such operational scenarios will be requested more frequently. Figure 3 illustrates some of these issues. At the top an overview over the whole discharge is shown. The stabilisation of the NTM is seen in the upper time trace. As the NTM is stabilized the amplitude becomes so small that the locking is lost. The box average of the gyrotron power shows that during modulation the duty cycle is ≈50 % changing to almost 100 % as noise creates only occasional triggers [1]. Further insight into the triggering requires a strong zoom (middle). At this zoom level it can be seen how other MHD disturbances (here ELMs) affect the triggering. They can suppress the zero crossings due to the NTM oscillation thereby blinding the phase detection algorithm on the FPGA for some periods resulting in a loss of ≈ 2% of the NTM oscillations for these specific conditions. A further zoom allows to check the phase shifts. As mentioned above, the shift between the top (green) and middle (red) curve can be adjusted at the phase shifter but the time shift between middle and lower curve is fixed (18 μs).

Acknowledgement

This project has received funding from the Euratom research and training programme 2014-2018

[1] The reason to have as a default 'full power' lies in the technical realization of the fast high-power modulation. The input power to the series modulator does not vary, but all power which is not output to the gyrotron during modulation is cooled away by the anode cooling of the modulator tetrode. The default 'full power' therefore protects the tetrode. In principle DCS could request to fully switch off the gyrotron (i.e. to apply a blocking voltage to the tetrode control grids) after it has detected a stabilisation of the mode, but this was not yet attempted.

References

[1] W. Kasparek et al., *Development of Resonant Diplexers for high-power ECRH - Status, Applications, Plans* (2014), these conference proceedings

[2] E. Poli et al., *On the criteria guiding the design of the upper electron-cyclotron laucher for ITER* (2014), these conference proceedings

[3] K. Behler, H. Blank, A. Buhler, R. Cole, R. Drube, K. Engelhardt, H. Eixenberger, N. Hicks, A. Lohs, K. Lüddecke et al., Fusion Engineering and Design **85**, 313 (2010)

[4] M. Reich, K. Behler, R. Drube, L. Giannone, A. Kallenbach, A. Mlynek, J. Stober, W. Treutterer, ASDEX Upgrade team, Fusion Science and Technology **58**, 727 (2010)

[5] W. Kasparek, B. Plaum, C. Lechte, E. Filipovic, V. Erckmann, G. Grünwald, F. Hollmann, M. Maraschek, G. Michel, F. Monaco et al., EPJ Web of Conferences **32**, 04008 (2012)

[6] J. Stober, D. Wagner, L. Giannone, F. Leuterer, F. Monaco, M. Maraschek, A. Mlynek, M. Münich, E. Poli, M. Reich et al., *ECRH on ASDEX Upgrade - System extension, new modes of operation, plasma physics results*, in *Electron Cyclotron Emission and Electron Cyclotron Resonance Heating (EC-16): Proceedings of the 16th Joint Workshop*, edited by R. Prater (World Scientific Publishing Co., Singapore, 2011), pp. 28–41, ISBN 978-981-4340-26-7

[7] J. Stober, A. Bock, H. Höhnle, M. Reich, F. Sommer, W. Treutterer, D. Wagner, L. Gianone, A. Herrmann, F. Leuterer et al., EPJ Web of Conferences **32**, 02011 (2012)

[8] M. Reich, A. Bock, M. Maraschek, ASDEX Upgrade Team, Fusion Science and Technology **61**, 309 (2012)

[9] L. Giannone, M. Reich, M. Maraschek, E. Poli, C. Rapson, L. Barrera, R. McDermott, A. Mlynek, E. Poli, Q. Ruan et al., Fusion Engineering and Design **88**, 3299 (2013)

[10] E. Poli, A. Peeters, G. Pereverzev, Comp. Phys. Comm. **136**, 90 (2001)

[11] A. Mlynek, M. Reich, L. Giannone, W. Treutterer, K. Behler, H. Blank, A. Buhler, R. Cole, H. Eixenberger, R. Fischer et al., Nuclear Fusion **51**, 043002 (2011)

[12] M. Reich, L. Barrera-Orte, K. Behler, L. Giannone, M. Maraschek, E. Poli, C. Rapson, J. Stober, W. Treutterer, ASDEX Upgrade team, *NTM stabilization experiments at ASDEX Upgrade*, in *Europhysics Conference Abstracts (CD-ROM, Proc. of the 40th EPS Conference on Plasma Physics, Espoo, Finland, 2013)*, edited by V. Naulin, C. Angioni, M. Borghesi, S. Ratynskaia, S. Poedts, T. Donné, T. Kurki-Suonio, S. Äkäslompolo, A. Hakola, M. Airila (European Physical Society, Geneva, 2013), Vol. 37D of *ECA*, p. P2.151, http://ocs.ciemat.es/EPS2013PAP/pdf/P2.151.pdf

[13] C. Rapson, L. Giannone, M. Maraschek, M. Reich, J. Stober, W. Treutterer, ASDEX Upgrade Team, Fusion Engineering and Design (2014), in Press

[14] H. van den Brand et al., *Detection of MHD instabilities with ECE* (2014), these conference proceedings

[15] M. Maraschek, G. Gantenbein, Q. Yu, H. Zohm, S. Günter, F. Leuterer, A. Manini, ECRH Group, ASDEX Upgrade Team, Physical Review Letters **98**, 025005 (2007)

[16] J. Stober, O. Gruber, A. Herrmann, M. Hirsch, H. Höhnle, W. Kasparek, F. Leuterer, M. Maraschek, F. Monaco, R. Neu et al., *Improved H-mode operation in fully W-coated ASDEX Upgrade - new demands for Electron Cyclotron Resonance Heating*, in *Europhysics Conference Abstracts (CD-ROM, Proc. of the 36th EPS Conference on Plasma Physics, Sofia, Bulgaria, 2009)*, edited by M. Mateev, E. Benova (European Physical Society, Geneva, 2009), Vol. 33E of *ECA*, pp. P–1.164, http://epsppd.epfl.ch/Sofia/pdf/P1_164.pdf

[17] M. Maraschek, Nuclear Fusion **52**, 074007 (2012)